

Modelling of accelerated cladding degradation in air for severe accident codes

C. Bals¹, E. Beuzet², J. Birchley³, O. Coindreau⁴, S. Ederli⁵, T. Haste³, T. Hollands⁶,
M. K. Koch⁶, J.-S. Lamy², K. Trambauer¹

CONTRACT SARNET FI6O-CT-2004-509065

- 1) GRS, Garching bei München (D)
- 2) EDF R&D, Clamart (F)
- 3) PSI, Villigen (CH)
- 4) IRSN DPAM/SEMCA, Cadarache (F)
- 5) ENEA, Roma (I)
- 6) RUB-LEE, Bochum (D)

Summary

The interaction of air-containing atmospheres with Zircaloy cladding can strongly affect the evolution of severe accident scenarios such as loss of water from a spent fuel pool or reactor pressure vessel breaching. Air ingress can lead to an accelerated oxidation of Zircaloy and hence faster core degradation, which in turn results in fuel oxidation and enhanced fission product release, most notably ruthenium. It is consequently of great importance to understand the phenomena governing oxidation of Zircaloy by air as a prerequisite to addressing the source term issues.

A state-of-the-art review performed before SARNET showed a high degree of variation among the existing kinetic data regarding zirconium alloy oxidation in air. New experimental programs comprising small-scale tests have therefore been launched at FZK, IRSN (MOZART program in the frame of the International Source Term Program – ISTP) and INR. A synthesis of the results, comparing them in terms of kinetics and oxide scale structure and composition has been reported in the previous ERMSAR meeting.

The data contribute to a better understanding of the oxidation process, especially regarding the role of nitrogen and highlight some important features that need to be taken into account in models for air oxidation. In particular it is observed that after a certain exposure time the reaction gives way to a much higher oxidation rate involving degradation of the oxidised cladding and strong breakaway effects, which are being included in models recently proposed and currently being incorporated into severe accident codes. This paper presents the main achievements performed in ATHLET-CD, ICARE/CATHARE, MAAP and MELCOR including a comparison between experimental and theoretical results.

A. INTRODUCTION

Before the EU 6th framework SARNET project, most of the severe accident codes used parabolic kinetics for air oxidation of Zircaloy and there was no treatment of nitriding. The weight gain correlations of Zircaloy claddings oxidized in air were based on the recommendation of the OPSA report {she-99-oxi} (see Fig 1). It was thus assumed that a protective oxide scale is built up and controls the progress of the reaction by oxygen diffusion through the oxide. The acceleration of the reaction rate (breakaway) due to the transition towards non-protective scales was not treated.

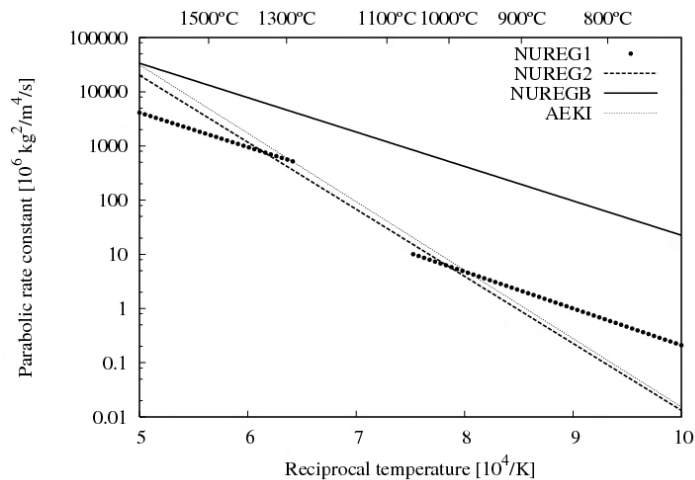


Fig 1: Correlations for the parabolic rate constant recommended in the OPSA report {she-99-oxi}

Recent separate-effect test campaigns performed at IRSN, FZK and INR within the SARNET project and the International Source Term Programme (ISTP) have been carried out {dur-07-sep}. They have shown that oxidation in air as well as in air and nitrogen-containing atmospheres leads to strong degradation of the cladding material. The main mechanism for the degradation process under the influence of nitrogen is formation of zirconium nitride and its re-oxidation. The different densities of Zr, ZrO₂, and ZrN cause volume mismatches, compressive stress build-up and relief by crack formation, associated with zirconia phase transformation, leading to porous, non-protective oxide scales. It results in fast progression of the oxidation front, as well as strong macroscopic deformation of the cladding. Kinetic data regarding the pre-breakaway parabolic regime, the mass gain at transition and the high oxidation rate in the post-breakaway regime have also been provided.

The Zircaloy/air oxidation modeling by parabolic kinetics is not sufficient to capture all relevant physical processes, and in particular the accelerated oxidation of the Zircaloy claddings that can occur under air conditions. Therefore, improved Zircaloy/air oxidation models are being developed in severe accident codes and are presented in the next paragraphs.

B. MODELING IN ATHLET-CD

The chemical equation of Zircaloy oxidation with the oxygen contained in air results in an exothermal energy of $\Delta h_{\text{Air}} = 1.2065 \cdot 10^7 \text{ J/kg}_{(\text{Zr})}$ which is about two times the value resulting from Zircaloy oxidation in steam atmosphere. Oxidation in air is calculated on the basis of the analytical solution of the diffusion equation. Similar as the oxidation with steam the reaction starts with parabolic kinetics given by the equation :

$$(1) \quad dm'/dt = R_i(T) / m'$$

for the formation of ZrO_2 where m' is the mass of oxidized Zirconium per surface area in kg/m^2 . At an oxide layer thickness which is defined by input data (standard value 0.25 mm) a transfer to linear kinetics is made. This has the effect that a further increase of oxide mass is not considered on the right side of equation (1) to simulate the effects of cracking and breakaway observed in the experiments {dur-2007-sep}.

The reaction rate R_i which is needed for the solution of equation (1) is described by an Arrhenius type equation :

$$(2) \quad R_i = A_i \cdot e^{(-E_i/T)} \cdot g(p_{\text{O}_2}) \cdot F_{\text{lim}}$$

where i selects the empirical correlation with A_i and E_i as defined in Tab. 1; $g(p_{\text{O}_2})$ is a function of the oxygen partial pressure (see equ. 3) and considers oxygen starvation. F_{lim} is an input value which could be used as a preliminary compensation for the up to now unavailable nitrid formation model but was set to 1 in the validation calculation of QUENCH-10 experiment. Fig. 2 shows the resulting reaction rates for the 8 options (i) available in ATHLET-CD. Some of the correlations need an interpolation between different temperature regimes; to get a linear transfer in the logarithmic diagram $R_i = f(1000/T)$ the interpolation functions were also defined as an additional Arrhenius function.

Tab. 1: Empirical correlations available in ATHLET-CD

	Correlation	A_i ($\text{kg}_{\text{Zr}}^2/\text{m}^4/\text{s}$)	B_i (K)	Range
1	Powers	10.50 $7.976 \cdot 10^{14}$ 50.40	15630.0 57180.0 14630.0	$T < 1300 \text{ K}$ interpolation $T > 1400 \text{ K}$
2	CODEX AIT1	428.1	17597.0	
3	NUREG2	$25.115 \cdot 10^4$	28485.0	
4	NUREG2 \rightarrow NUREG1	$25.115 \cdot 10^4$ $5.807 \cdot 10^7$ 50.40	28485.0 34860.0 14630.0	$T < 1180 \text{ K}$ interpolation $T > 1450 \text{ K}$
5	NUREG2 \rightarrow CODEX AIT1	$25.115 \cdot 10^4$ $5.47 \cdot 10^{26}$ 428.1	28485.0 80320.0 17597.0	$T < 1055 \text{ K}$ interpolation $T > 1130 \text{ K}$
6	AEKI – Mixture Ar and O_2	$2.55 \cdot 10^4$ 74.80	25792.0 17895.0	$T < 1353 \text{ K}$ $T > 1353 \text{ K}$
7	AEKI – Air (IRSN, corr.fac.10)	$2.735 \cdot 10^5$	29054.0	
8	ICARE/CATHARE - Air	10.50 $2.512 \cdot 10^5$ 50.40	15630.0 28470.0 14627.0	$T < 1265 \text{ K}$ interpolation $T > 1625 \text{ K}$

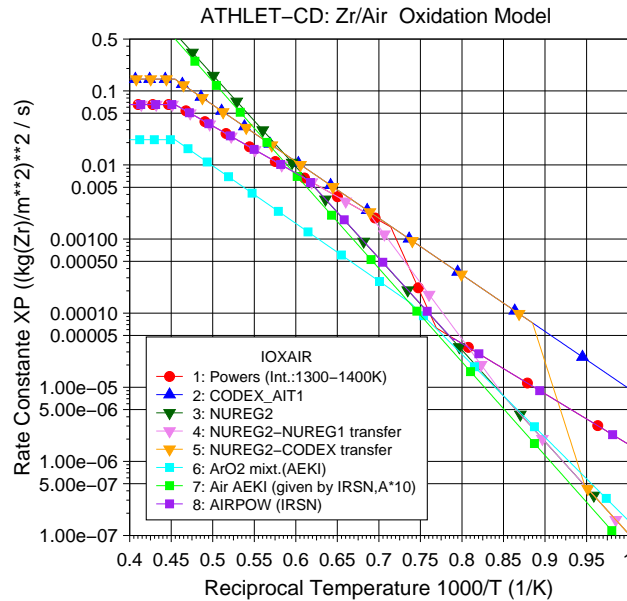


Fig. 2: Available correlations for Zr/Air oxidation in ATHLET-CD

Corresponding to the consideration of steam starvation the factor $g(p_{O_2})$ is calculated as

$$(3) \quad g(p_{O_2}) = (10 - (15 - 6 \cdot f_p) \cdot f_p) \cdot f_p^3$$

with $f_p = (p_{O_2} / p) / x_{lim}$ and the limitation $0 \leq g(p_{O_2}) \leq 1$, where p_{O_2} is the partial pressure of oxygen, p is the total pressure of the steam / gas mixture and x_{lim} is the upper limit of p_{O_2} / p to start the reduction to values below 1. This polynomial of 5th degree for f_p provides a smooth and steady stop or activation of the air oxidation reaction during a transfer into or out of an oxygen starvation phase. The recommended region to initiate the reduction is $0.01 \leq x_{lim} \leq 0.1$.

From the measured development of the hydrogen production a preferred oxidation of Zircaloy with oxygen in an air-steam mixture was identified. As a consequence of this experimental behavior the rate of steam oxidation is multiplied by a factor $r_{vap,ox}$ which regards the partial pressure of oxygen in a mixture. For oxygen pressure fractions p_{O_2} / p between 10^{-4} and 10^{-2} $r_{vap,ox}$ varies between 1 and 0, so that the oxidation of steam during a phase of air oxidation can be eliminated dependent on the oxygen partial pressure.

With equation (1) the mass of Zirconium dm_{Zr} , which is oxidized in time step dt can be calculated from $dm' \cdot A$ where A is the available surface area for the oxidation at the beginning of the time step. At the end of the time step the actual Zirconium mass consumption dm_{Zr} is added to the total mass of oxidized Zr and from that the actual thickness of the oxide layer at time t will be calculated, taking into account the different densities of Zr and ZrO_2 .

Proportional to the consumed metallic Zr the exothermal energy is considered as heat source of the cladding and the consumed oxygen is considered as a mass sink of the thermofluid dynamic system.

As shown above the air ingress model of ATHLET-CD considers the oxygen of the air only. Therefore the model will be improved by implementing the reaction of the nitrogen of the air with the zirconium under defined boundary conditions like the steam and oxygen starvation, the existence of zirconia and the thickness of the zirconia layer.

C. MODELING IN MAAP

For performing PSA Level 2 studies, a short computational time is needed. Cladding air oxidation is consequently modelled with cladding weight gain, rather than Fick equations {bac-2005-des}.

In accordance with the overall literature {she-99-oxi} and {coi-07-air}, several correlations for cladding air oxidation are available in MAAP (table 2).

Weight gains are described by Arrhenius function : $K=A_i \cdot \exp(-B_i/T)$

The breakaway is given by a parameterized temperature criterion, defined on the transformation of zirconia (1447K) or by a criterion based on the weight gain and specified by IRSN during MOZART experiments.

Tab. 2: Correlations available in MAAP

Correlations	$A_i(\text{kg}_{\text{Zr}}^2/\text{m}^4/\text{s})$	$B_i(\text{K})$	Range
NUREG [pow-94]	10.50	15630	$T < 1333\text{K}$
	$25.11 \cdot 10^4$	28485	$1333\text{K} \leq T \leq 1550\text{K}$
	50.40	14634	$T > 1550\text{K}$
CODEX	428	15597	$\forall T$
ANL pre-breakaway (pre-oxidised clads)	26.82	17490	$\forall T$
ANL post-breakaway (pre-oxidised clads)	2982.27	19680	$\forall T$
ANL pre-breakaway (unworked clads)	65.82	18620	$\forall T$
AEKI	$21.72 \cdot 10^4$	29054	$\forall T$
Combined (ANL pre-breakaway (pre-oxidised clads) then JAERI)	26.82	17490	$< 1447\text{K}$
	0.898	13780	$\geq 1447\text{K}$
ICARE/CATHARE (from MOZART)	$2.27 \cdot 10^4$	23442	$< 92.96 \exp(-7024.3/T)$
	261.63	15937	$> 92.96 \exp(-7024.3/T)$ [coi-07-air]

The post-breakaway regime can be simulated by parabolic or linear correlations, even if experimental findings recommend linear.

If both steam and oxygen are available, oxidation is done before with oxygen. The Zr oxidation model in MAAP only takes into account the oxygen of the air. We expect to improve this model by implementing the reaction with nitrogen.

With regard to QUENCH 10 experiment, we have chosen parabolic correlations before and after breakaway. This choice can be justified by the experimental findings from the FzK separated tests. They show air oxidation is not accelerated when claddings have been pre-oxidised during a long time and at high temperature [ste-08-oxi] (for instance nearly 2h and $> 1600\text{K}$ in QUENCH10 experiment). The oxide thickness is consequently thick and protective.

D. VALIDATION OF ATHLET-CD AND MAAP AGAINST QUENCH 10

The test QUENCH-10 was performed at Forschungszentrum Karlsruhe (FZK) to investigate the bundle behaviour during air ingress conditions and during flooding of the degraded core by water afterwards {sch-2006}. The QUENCH facility essentially consists of the out-of-pile bundle. This bundle includes 20 heated rods, 1 unheated central rod, which could be used for measurement devices or as a control rod, as well as 4 corner rods.

The 21 simulator rods have a length of about 2.5 m, while approximately 1 m of the heated rods is electrically heated. For the experiment as well as for the calculations the beginning of the heated length is defined as height 0 m. The tungsten heaters (outer diameter: 6 mm) are surrounded by annular pellets made of ZrO₂ simulating the fuel pellets, which are bordered by Zircaloy-4 claddings (outer diameter: ~ 11 mm). The 21 rods and the 4 corner rods are arranged in a 5x5 matrix. To be able to detect fuel rod failure the heated rods are filled with argon-krypton or helium, which can be measured by a mass spectrometer. The 4 corner rods made of Zircaloy are implemented for additional thermocouple instrumentation as well as to allow the measurement of the axial oxide layer profile by withdrawal the corner rods at different point of times during the test performance {ste-2005}

After a stabilisation phase at the beginning (~ 873 K during ~600s) the bundle of QUENCH-10 was heated up to a temperature of about 1623 K (during ~2000s) before the bundle was pre-oxidised by super heated steam for nearly 9700s. During pre-oxidation the temperatures increased only up to app. 1700 K and an oxide layer thickness of about 500 µm was built-up. In the intermediate cooldown phase the bundle was cooled by reducing the electrical power and the temperatures decreases to app. 1183 K during 2300s. A first corner rod was withdrawn. The air ingress was initiated afterwards by an air feed of 1 g/s (23 % O₂, 77 % N₂) during 1800s. The steam flow was shut down during this phase. Because of the exothermal reaction of the oxygen and the zirconium the temperatures increased and reached a temperature of app. 2200 K. A second corner rod was withdrawn and an oxide layer of about 600 µm was measured. The final cooldown or quenching phase was initiated by the shut down of the air feed and by flooding the bundle with water of app. 50 g/s {sch-2006} during 300s.

The modelling of the test facility and the implemented initial and boundary conditions differs in the SA codes ATHLET-CD and MAAP mainly in the modelling of the core. While the 21 simulator rods are summarised to three rings (1 unheated rod, 8 heated rods and 12 heated rods) in ATHLET-CD using 20 axial nodes (5 for the lower plenum, 10 for the heated zone and 5 for the upper plenum), the modelling in MAAP considers 3 rings (1 unheated rod + 4 heated rods, 8 heated rods and 8 heated rods) and 58 axial meshes (5 for the lower plenum, 48 for the core and 5 for the upper plenum). For the calculation using ATHLET-CD and MAAP, the components rods, shroud and grids are modelled.

In the calculations using ATHLET-CD the Zr-H₂O reaction is calculated by the correlations of Cathcart and Prater/Courtright and the reaction of the oxygen from the air with zirconium is calculated by the correlations of Powers (cp. Fig. 2 and Tab. 1 of the §B. Modelling in ATHLET-CD). For the MAAP calculations the correlations of Cathcart and Urbanic are used for the Zr-H₂O reaction and the correlations NUREG1 and NUREG2 {she-99-oxi} are used for the reaction during air ingress.

The thermal behaviour of the bundle given in Fig. 3 shows a good agreement to the experimental data for both codes. The calculated temperatures with ATHLET-CD are a little bit lower than in the calculation with MAAP, but the increase starts earlier than in the

calculations with MAAP. For the comparison between the experiment and the calculations with ATHLET-CD and MAAP the measurement device TFS 2/11 is considered up to 13326 s when it failed and afterwards the thermocouples of the shroud (TSH 11/0 and TSH 11/180) are used. The level of the temperature of the shroud is a little bit lower, but can give an indication of the thermal behaviour of the bundle.

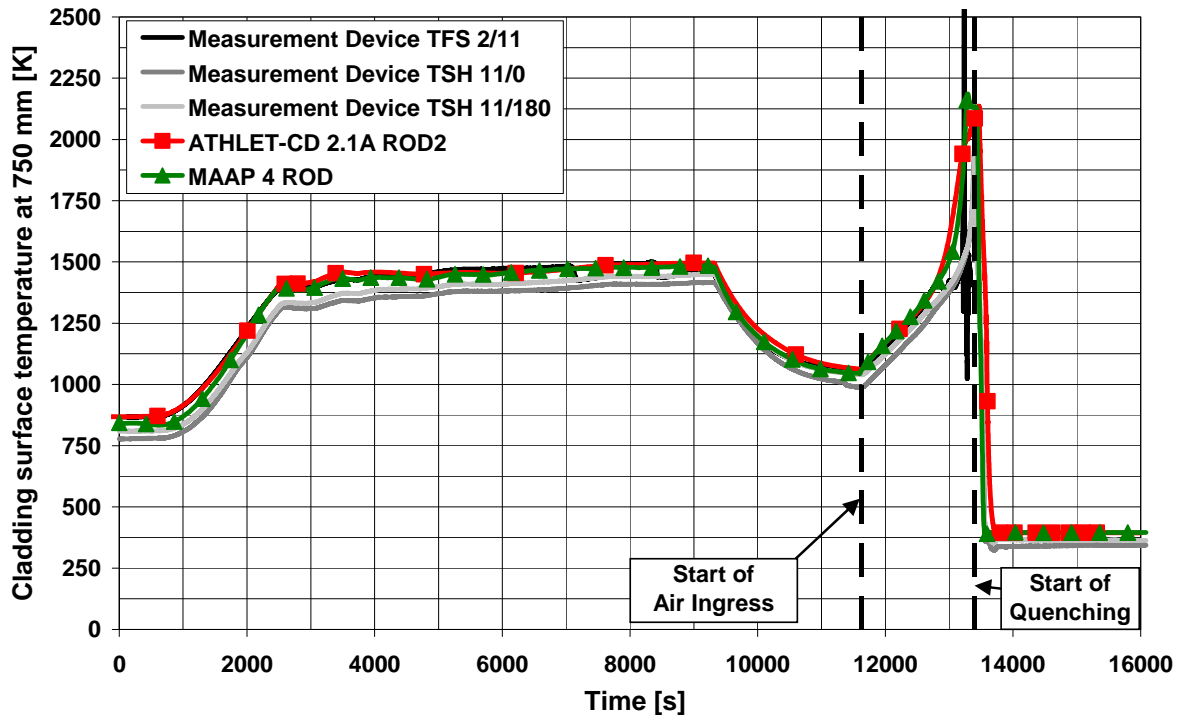


Fig. 3: QUENCH-10 measured and calculated temperatures, by ATHLET-CD and MAAP, on 750 mm bundle height

During the second half of the air ingress phase the course of the temperatures in the ATHLET-CD calculation is based on a too high calculated oxidation so that the exothermal heat input coming from the oxidation is too high. The over-predicted oxidation can be seen in Fig. 4, too, where the oxygen consumption during the air ingress phase is shown. While the qualitative behaviour is calculated quite well with a slight under-prediction at the beginning, the quantitative course shows that the over-estimation of the oxygen consumption occurs at the end of the air ingress phase. An oxygen consumption of about 93 g is calculated by ATHLET-CD which represents an over-estimation of nearly 11 % in comparison to the measured value of app. 84 g. Most of the consumed oxygen from the air is calculated for the bundle itself (~ 89 g), while the shroud and the grids dissipate only 4 g of oxygen.

In the calculations using MAAP, the qualitative behaviour of the oxygen consumption is calculated quite well. It shows an overall mass of O₂ of app. 73 g. The overall calculated mass consumed represents 87% of the measured 84 g. The slight under-prediction of the oxygen consumption comes probably from the use of parabolic correlations during the overall simulation and a criterion defined on the transformation from tetragonal to monoclinic zirconia that do not lead to a temperature escalation as quick as the experiment. Parabolic correlations were chosen because of the long pre-oxidation phase and the thick oxide layer.

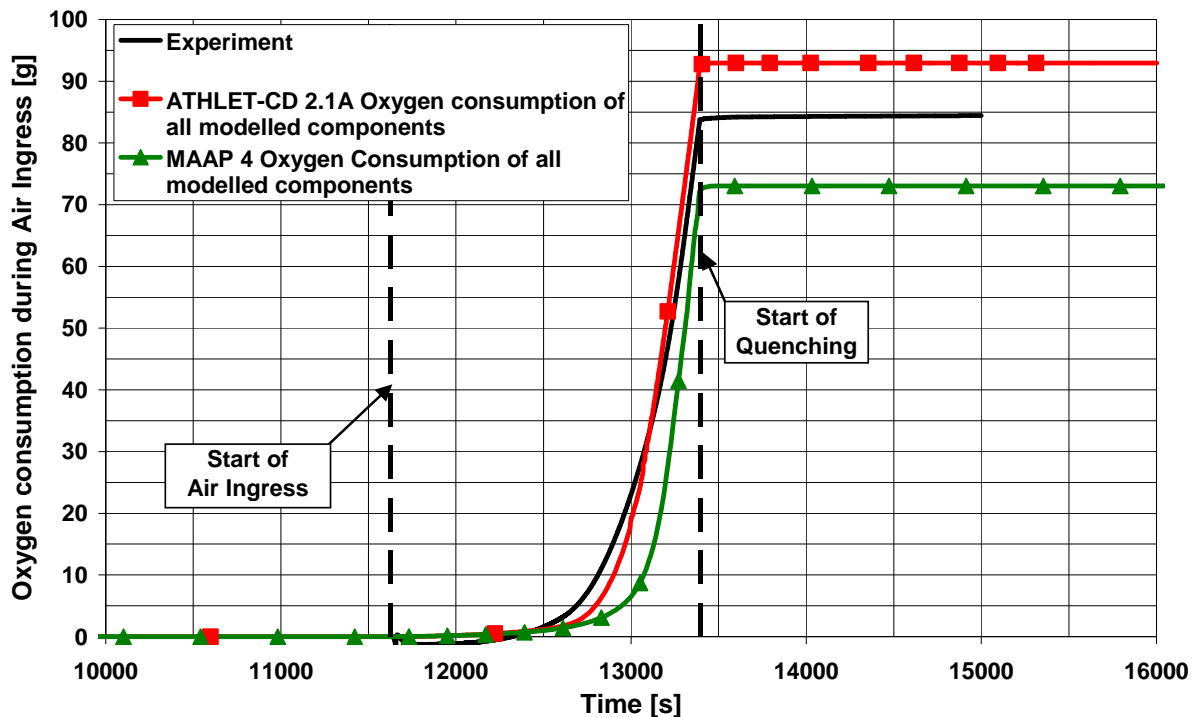


Fig. 4: QUENCH-10 calculated oxygen consumption during air ingress of the SA codes, ATHLET-CD and MAAP, versus experimental data

The calculated thermal behaviour during the air ingress phase has direct impact on the temperatures and corresponding to them on the hydrogen generation in the quench phase (Fig. 5). In MAAP the calculated temperatures are a bit lower compared to ATHLET-CD because of lower temperatures after the air ingress what leads to a small amount of hydrogen of about less than 1 g in addition to the app. 26.4 g H₂ after the intermediate cooldown. In the calculations using MAAP, the overall calculated mass of hydrogen of app. 27.2 g from the model is under-predicted and represents only 52 % of the measured 53 g H₂ during QUENCH-10, but the qualitative behaviour of the hydrogen generation is predicted well. The under-prediction of H₂ production at the end comes from its under-prediction during pre-oxidation and from lower temperatures at the end of air ingress. The reason remains in the fact that shroud and grids are not modelled as fine as rods are, because they are not taken into account in reactors. Without grids and shroud models in MAAP, we implemented simplified ones which under-estimate oxidizable surfaces. The qualitative course of the H₂ production in the calculations using ATHLET-CD is predicted in good agreement to the experimental data and show only a small over-estimation of the overall hydrogen generation of 6 %. The amount of H₂ (~ 48 g) up to the end of the end of the air ingress phase is calculated in good agreement to the experiment, while the hydrogen generation during quenching of app. 8 g is overestimated, because of the too high calculated temperatures during the air ingress.

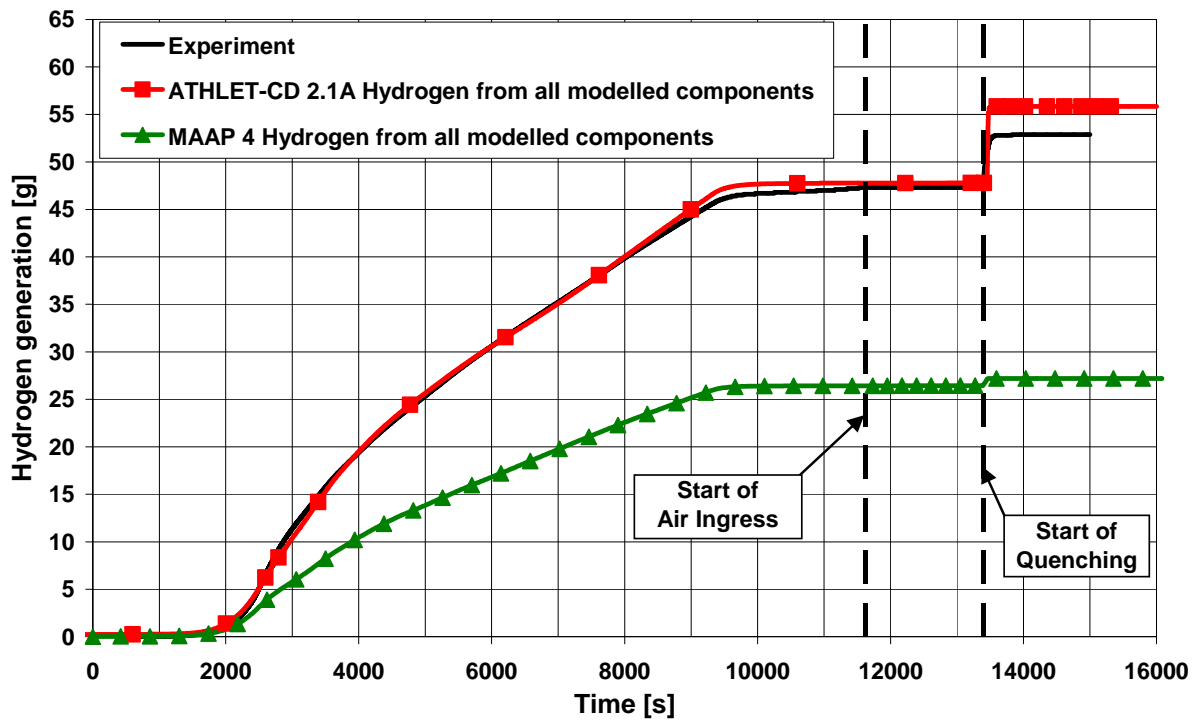


Fig. 5: QUENCH-10 calculated hydrogen generation, by ATHLET-CD and MAAP, versus experimental data

The validation of both codes show in general a good agreement to the experiment concerning the thermal behaviour up to the end of the intermediate cooldown, but during the air ingress phase the calculations varies from the measurement data. This leads to further demand of the physical understanding and corresponding to that to the modelling of the phenomena of the air ingress. For example the influence of nitride formation is not included in ATHLET-CD and MAAP yet, but it has an impact on the cladding and the thermal behaviour in the case of re-oxidation when oxygen is available again after an oxygen starvation phase {dur-2007-sep}.

E. MODELING IN ICARE/CATHARE AND VALIDATION AGAINST MOZART SET

Developments in the ICARE/CATHARE v2 code regarding air oxidation include the treatment of oxygen starvation, the formation of ZrN in case of total oxygen starvation and the simulation of breakaway effects with the transition from parabolic to accelerated kinetics. A description of the improved air oxidation model that takes into account breakaway transition is given hereafter. Then, a comparison of the weight gain measured in the MOZART experiments and calculated with the standard and the improved air oxidation model is presented.

In the pre-transition regime, the total weight gain is described by a parabolic law (Eq. 4).

$$(4) \quad \frac{d(\Delta m/S)^2}{dt} = K_p$$

This is actually a first approximation since departures from parabolic to subparabolic kinetics were observed a long time ago {eva-72-cri, dou-71-zir} and were also observed in

recent experiments. They can be attributed to the increase of compressive stress with time or to a reduction of diffusion path density in the scale with time.

Several correlations for the parabolic scaling rate K_p are available, in particular the NUREG1-2 {pow, 1994}, the NUREGB {she-1999-oxi}, the AEKI {she-1999-oxi} and the MOZART correlation, derived from the MOZART program with $K_p [\text{kg}^2 \text{m}^{-4} \text{s}^{-1}] = 696.75 \exp(-1.949 \times 10^5 / RT)$.

The MOZART program has shown that the breakaway transition occurs for a critical value of weight gain which is strongly temperature dependent. Moreover, the weight gain at transition can be correlated to the temperature by a hyperbolic law (see Eq. 5), which is supported by the assumption that the breakaway transition is linked with transformation of tetragonal to monoclinic zirconia. The oxide formed between 600°C and 1150°C is expected to be monoclinic zirconia (noted m-ZrO₂) but tetragonal zirconia (noted t-ZrO₂) can also be found, being stabilized at subcritical temperatures by fine grain size, hydrostatic pressure, or a very high defect concentration {dou-71-zir}. The presence of tetragonal zirconia in the oxide scale is generally attributed to high compressive stresses {god-94-how} and it was shown by Raman spectroscopy {god-98-str} that compressive stresses in the oxide layer are larger at the metal-oxide interface and reduce away from this interface. It can thus be conjectured that the compressive strain energy is largest near the Zr/ZrO₂ interface (where compressive stresses are maximum) and decrease away from the interface (due to the decrease of compressive stresses). As the oxide grows the compressive strain-energy at the oxide-gas interface decreases. When the oxide reaches a critical thickness, the compressive strain energy is not high enough to keep the tetragonal phase stable. The thermodynamically stable m-ZrO₂ tends to form upon the surface of t-ZrO₂. Due to its larger volume, the m-ZrO₂ stresses the underlying t-ZrO₂ causing extensive crack formation and propagation. The breakaway can thus be thought to be related to the tetragonal-monoclinic transformation of ZrO₂ accompanied by crack formation. The formation of m-ZrO₂ is possible when the free energy change of t-ZrO₂ to m-ZrO₂, $\Delta G(t \rightarrow m)$, given by :

$$\Delta G(t \rightarrow m) = G_m^0(T) - G_t^0(T) + (u_m - u_t)$$

$$\text{with } \begin{cases} G_m^0(T), G_t^0(T) : \text{standard free energy of m-ZrO}_2 \text{ and t-ZrO}_2 \text{ formation in J/mol} \\ u_m, u_t : \text{compressive strain energy of m-ZrO}_2 \text{ and t-ZrO}_2 \text{ in J/mol} \end{cases}$$

becomes lower or equal to 0.

Assuming that the strain-energy difference between the monoclinic and the tetragonal phase decreases with the mass gain according to equation: $u_m - u_t = A/(\Delta m / S)^B$ and considering that the free energy difference can be approximated by: $G_m^0(T) - G_t^0(T) = H_{tr}(1 - T/T_b)$

$$\text{where } \begin{cases} H_{tr} = -5.94 \times 10^3 \text{ J/mol is the enthalpy of transformation of t-ZrO}_2 \text{ to m-ZrO}_2 \\ T_b = 1447 \text{ K is the temperature of transformation of m-ZrO}_2 \text{ to t-ZrO}_2 \end{cases}$$

the critical mass gain at breakaway corresponds to: $A/(\Delta m / S)_{break}^B = -H_{tr}(1 - T/T_b)$.

Experimental weight gains at transition determined experimentally in the MOZART program were used to determine the A and B coefficients and the following correlation was obtained:

$$(5) \quad (\Delta m / S)_{break} = 3.19 \times 10^5 (T_b / H_{tr} (T - T_b))^{2.27328}$$

After the breakaway transition, a much higher scaling rate is observed. This accelerated kinetics can be described by Eq. (6):

$$(6) \quad \frac{d(\Delta m / S)^{0.5}}{dt} = K_a \quad \text{with } K_a [kg^{0.5} m^{-1} s^{-1}] = 45.9 \exp(-1.325 \times 10^5 / RT)$$

The MOZART experimental set-up has been modelled using ICARE/CATHARE. The modelling is mono-dimensional, with 10 axial meshes and one fluid channel. Comparisons between experimental and numerical results are shown in Fig 6. The standard air oxidation model largely overestimates the time for complete oxidation whereas the improved air oxidation model provides a much better agreement. Results obtained with the improved model are discussed hereafter:

- At low temperature (600-700°C), there is a rather good agreement between measured and computed mass gain. Time at breakaway transition is satisfactorily reproduced by the model. After breakaway transition, the slopes of the experimental and numerical plots are slightly different. This is due to the modelling of the post-breakaway kinetics by an accelerated law whereas a roughly linear kinetics is observed.
- At 800-850°C, there is a good agreement between observed and computed mass gain. The accelerated kinetic regime is well reproduced.
- At 900°C, time to reach complete oxidation is underestimated (150 minutes in the calculation and more than 200 minutes in experiment). The breakaway transition occurs too early compared to experiment (after 20 minutes in experiments and only 13 minutes in simulations). Actually, the determination of the experimental time at transition is difficult since the oxidation rate stays around its minimum value during about 30 minutes. Time at breakaway was determined on the experimental curve when the oxidation rate stops decreasing. However, the accelerated regime does not start at this moment but 30 minutes later, when the oxidation rate starts to increase again. In the simulation, this delay is not taken into account and the accelerated regime occurs too early. This is the main source of error since there is quite good agreement between the observed and the modelled accelerated scaling rate.
- At 1000°C, there is a good agreement between experiment and simulation and time for complete oxidation is well reproduced by the model. The breakaway transition is observed after 14 minutes in experiments and between 20 (in meshes close to air inlet) and 60 minutes (in the vicinity of outlet region) in simulations. This means that in spite of a relatively high air flow rate (500 ml/min), local starvation conditions are reached, leading to an inhomogeneous scale growth. In the simulation, the oxide layer is thicker close to the air inlet, where breakaway occurs at first. Breakaway propagates along the cladding leading to a kinetic transition that appears progressive at the macroscopic scale.

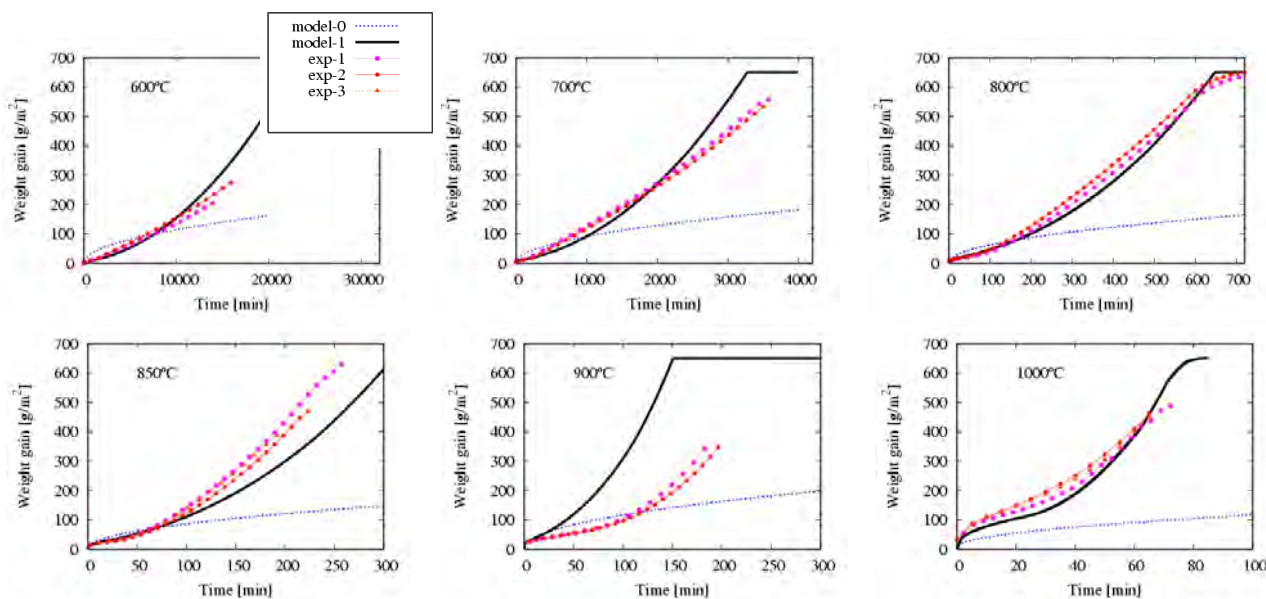


Fig 6: Comparison between MOZART experimental and ICARE/CATHARE calculated weight gain versus time. “model-0” refers to the standard air oxidation model (parabolic law) and “model-1” to the improved one (that takes into account breakaway transition)

F. MODELING IN MELCOR AND VALIDATION AGAINST FZK SET

In common with other plant analysis codes in current use, MELCOR adopts a parabolic model for air oxidation. Various correlations were reviewed {benj-1979} from which a single correlation known as NUREG-B was chosen as default in MELCOR in order to provide a conservative upper bound on the oxidation rate. An alternative correlation known as NUREG-A uses different kinetic parameter values in different temperature ranges and is considered to provide a better estimate of the oxidation rate. However, analysis of the air ingress test QUENCH-10 {birch-2004} revealed the limitations of the MELCOR model, with either the default correlation or alternative fits to data. In every case an immediate switch to the air oxidation model did not capture the gradual transition to faster kinetics.

PSI is therefore developing a model which seeks to represent the observed characteristics of air oxidation: faster kinetics under most conditions with a tendency toward linear kinetics, delayed or gradual transition to faster kinetics after pre-oxidation in steam, breakaway behavior of the oxide scale at low and moderate temperatures. The model development is being performed as part of an agreement between the Swiss Nuclear Safety Authority (HSK) and the USNRC. In order that the model can be developed, implemented and tested within a practical time-frame, and also remain within the overall spirit of MELCOR, a largely empirical approach is being adopted, based on results of separate effects experimental data. The main sources of data being used in the model development is the thermal balance (TB) tests at FZK and IRSN, while assessment will be performed using data not used in the development, e.g. BOX (FZK) and Argonne National Laboratories {nate-2004}, while QUENCH-10 data will be used for validation under transient conditions in a rod bundle

The TB tests provide transient data which is advantageous for model development. However, the present rig cannot be operated with steam, so that an oxygen-argon mixture is used as surrogate. Tests by Uetsuka and Hofmann {uet-hof-1985} indicate similar kinetics for oxygen and steam. The resulting correlation for oxygen is being used as the starting point for the air oxidation model and is similar to that of Cathcart-Pawel at the temperatures of main interest. The model is still undergoing development, so only a brief description is given to indicate the main characteristics and to illustrate the comparison with data. The model modifies the rate-limiting effect of the growing oxide layer by imposing a temperature-dependent upper bound, δ^* , on the effective oxide thickness. The kinetic model then takes the following form.

$$\text{Mass gain rate/area: } R = \rho(\text{Zr}) \frac{d(\delta)}{dt} = A \exp(-B/T) / \min(\delta, \delta^*)$$

where δ = oxide thickness.

A and B are Arrhenius constants and $\rho(\text{Zr})$ is the density of the cladding material. The upper bound δ^* is defined separately for air and steam, and in principle could depend also on the cladding material. It is applied progressively over a time period to represent the finite rate of transition. The case where δ^* is large reverts to the traditional parabolic model. It is assumed in MELCOR that the mass gain and thickness are directly linked according to the densities of metallic and stoichiometric oxide, and this relation is used in the model. Nitride formation is not represented at this stage. A virtue of this conceptually simple approach is that it practical to apply in a system-level code and offers flexibility to account for a wide range of conditions. The model for steam and air oxidation is indicated schematically in figure 7.

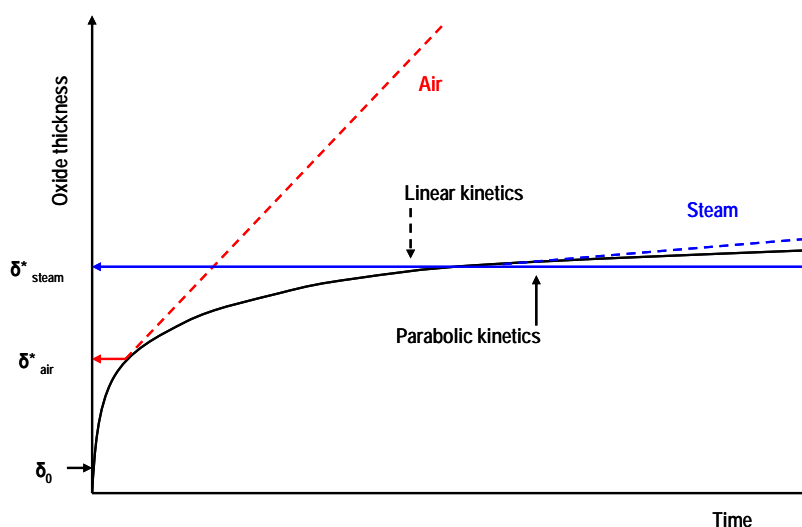


Fig 7: Schematic of MELCOR air oxidation model

Sample comparisons with FZK data are shown in figure 8 which illustrates the establishment of faster, linear kinetics at 800 °C in air, and the delayed transition to a similar rate following two different periods of pre-oxidation, while in oxygen the kinetic acceleration is a much milder. These trends are correctly captured in each case.

SESSION S2 (Corium) Paper N°2-4

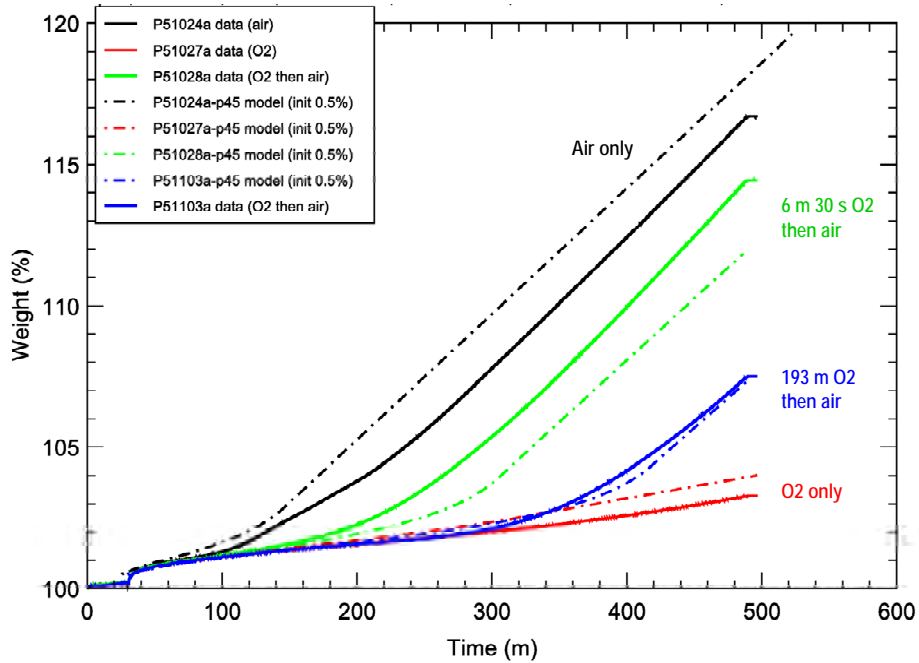


Fig 8: Comparison of MELCOR model with FZK data: oxygen + air oxidation at 800°C

G. COMPARISON BETWEEN THE DIFFERENT APPROACHES AND NEEDS FOR FURTHER DEVELOPMENTS

H. CONCLUSIONS

Acknowledgement

Regarding ATHLET-CD analyses performed by RUB-LEE, the authors give specific acknowledgement to the German Federal Ministry of Economics and Technology (BMWi 150 1305) for their sponsoring.

References

- {dur-07-sep} C. Duriez, M. Steinbrück, D. Ohai, T. Meleg, J. Birchley, T. Haste, "Separate-Effect Tests on Zirconium Alloy Cladding Degradation in Air Ingress Situations", 2nd European Review Meeting on Severe Accident Research (ERMSAR-2007), Forschungszentrum Karlsruhe GmbH (FZK), Germany, 12-14 June 2007
- {eva-72-cri} E. B. Evans and N. Tsangarakis, H.B. Probst, and N. J. Garibotti, Critical Role Of Nitrogen During High Temperature Scaling of Zirconium, Proc. Conf. Met. Society of AIME", pp. 248-282 (1972)
- {dou-71-zir} D.L Douglas, The metallurgy of zirconium, International Atomic Energy Agency, pp. 389-439 (1971)
- {she-99-oxi} I. Shepherd et al., Oxidation phenomena in severe accidents (OPSA), INV-OPSA(99)-P008, EUR 19528 EN (2000)
- {hay-49-som} E.T Hayes and A.H Roberson, Some effects of heating zirconium in air, oxygen and nitrogen, J. Electro-chem-Soc 142, pp. 142-151 (1949)
- {whi-67-aec} J.H. White, AEC Fuels and Materials Development program, Progress report, GEMP-67, General Electric Company (1967)
- {god-94-how} J. Godlewski, How the tetragonal Zirconia is stabilized in the oxide scale that is formed on a Zirconium alloy corroded at 400°C in steam, ASTM-STP 1245, pp. 663-686 (1994)
- {god-98-str} J. Godlewski, P. Bouvier, G. Lucazeau and L. Fayette, Stress distribution measured by Raman spectroscopy in zirconia films formed by oxidation of Zr-based alloys, ASTM-STP 1354, pp. 877-900 (1998)
- {pow-1994} D.A. Powers, L.N. Kmetyk, R.C. Schmidt, A Review of Technical Issues of Air Ingression during Severe Reactor Accidents, Report NUREG/CR-6218, SAND94-0731, Sandia National Lab.(1994)
- {benj-1979} A.S. Benjamin, D.J. McCloskey, D.A. Powers and S.A. Dupree, "Spent Fuel Heatup Following Loss of Water during Storage", NUREG/CR-0649 (1979)
- {birch-2004} J. C. Birchley and T. J Haste "Post-test Analysis of QUENCH-10 with MELCOR and SCDAP/RELAP5", Presented at the 10th International QUENCH Workshop, Karlsruhe (2004)
- {uet-hof-1985} H. Uetsuka and P. Hofmann, "Reaction Kinetics of Zircaloy-4 in a 25% O₂ / 75% Ar Gas Mixture from 900 to 1500 °C under Isothermal Conditions", KfK 3917 (1985)
- [nate, 2004] K Natesan and W K Soppet, "Air Oxidation Kinetics for Zr-based Alloys", NUREG/CR-5846, ANL-03/32 (2004).
- {sch-2006} G. Schanz, M. Heck, Z. Hozer, L. Matus, I. Nagy, L. Sepold, U. Stegmaier, M. Steinbrück, H. Steiner, J. Stuckert, P. Windberg: *Results of the QUENCH-10 Experiment on Air Ingress*, Wissenschaftliche Berichte, FZKA 7087, SAM.-LACOMERA-D09, Forschungszentrum Karlsruhe, Institut für Materialforschung, Programm Nukleare Sicherheitsforschung, Mai 2006.
- {ste-2005} M. Steinbrück, W. Hering, J. Stuckert, J. Birchley, E. Brunet-Thibault, T. Drath, N. Seiler, K. Trambauer, M.S. Veshchunov.: *Core reflooding: Synthesis of the QUENCH program and its impact on code modelling*, Proceedings of the 1st European Review Meeting

SESSION S2 (Corium) Paper N°2-4

on Severe Accident Research (ERMSAR-2005), Aix-en-Provence, France, 14-16 November 2005.

{bac-05-des} S. Bachere, F. Duplat, 'MAAP code description and validation', report ENTEAG030096A, 2005

{coi-07-air} O. Coindreau, S. Ederli, 'Air oxidation modeling in ICARE/CATHARE : a first improvement', SEMCA-2007-115, 2007

{ste-08-oxi} M. Steinbrück, 'Oxidation of Zircaloy-4 in atmosphere containing air and nitrogen', 5th Meeting of the ST OXIDEN, Ru Behaviour Circle, 30th of June 2008